Peer reviewed version of the manuscript published in final form at
https://doi.org/10.1089/ten.tea.2013.0304

Enhanced Osseous Implant Fixation with Strontium-Substituted Bioactive Glass Coating

Simon D. Newman,[1,+] Nasrin Lotfibakhshaiesh,[2,3,4,+] Matthew O'Donnell,[2,3] X. Frank Walboomers,[5] Nicole Horwood, [6] John A. Jansen, [5] Andrew A. Amis, [7] Justin P. Cobb,[1] and Molly M. Stevens,[2,3,*]

[+]Joint first authors.

1) MSk Lab, Imperial College London, Charing Cross Hospital, London, United Kingdom.
2) Department of Materials, Institute for Biomedical Engineering, Imperial College London, London, United Kingdom.
3) Department of Bioengineering, Institute for Biomedical Engineering, Imperial College London, London, United Kingdom.
4) Department of Tissue Engineering, School of Advanced Technologies in Medicine, Tehran University of Medical Sciences, Tehran, Iran.
5) Department of Biomaterials, Radboud University Medical Center, Nijmegen, Netherlands.
6) The Kennedy Institute of Rheumatology, University of Oxford, Oxford, United Kingdom.
7) MSk Lab, Department of Mechanical Engineering, Imperial College London, London, United Kingdom.

**E-mail:* m.stevens@imperial.ac.uk

ABSTRACT

The use of endosseous implants is firmly established in skeletal reconstructive surgery, with rapid and permanent fixation of prostheses being a highly desirable feature. Implant coatings composed of hydroxyapatite (HA) have become the standard and have been used with some success in prolonging the time to revision surgery, but aseptic loosening remains a significant issue. The development of a new generation of more biologically active coatings is a promising approach for tackling this problem. Bioactive glasses are an ideal candidate material due to the osteostimulative properties of their dissolution products. However, to date, they have not been formulated with stability to devitrification or thermal expansion coefficients (TECs) that are suitable for stable coating onto metal implants while still retaining their bioactive properties. Here, we present a strontium-substituted bioactive glass (SrBG) implant coating which has been designed to encourage peri-implant bone formation and with a TEC similar to that of HA. The coating can be successfully applied to roughened Ti6Al4V and after implantation into the distal femur and proximal tibia of twenty-seven New Zealand White rabbits for 6, 12, or 24 weeks, it produced no adverse tissue reaction. The glass dissolved over a 6 week period, stimulating enhanced peri-implant bone formation compared with matched HA coated implants in the contralateral limb. Furthermore, superior mechanical fixation was evident in the SrBG group after 24

weeks of implantation. We propose that this coating has the potential to enhance implant fixation in a variety of orthopedic reconstructive surgery applications.

Introduction

Rapid and reliable osseomechanical integration of devices is a highly desirable element of skeletal reconstructive surgery. Polymethylmethacrylate (PMMA) cement is often used to retain implants in the bone, but this technique is technically demanding for the surgeon to achieve long-term fixation, is associated with potentially fatal cardiopulmonary effects during implantation, and includes no direct interaction between implant and bone, thus introducing an additional interface that may fail.[1] The commonest approach to enhance implant fixation without the aid of cement is to coat implants with hydroxyapatite (HA), which conducts bone growth over the implant surface. Over the past 25 years, this has proved to be an effective technique in hip reconstructive surgery.[2] However, it has proved less successful in preventing revision surgery than PMMA in elderly patients undergoing total hip replacement or in ensuring reliable long-term survival of joint replacements in other anatomical locations such as the knee or ankle.[3,4] One method to potentially improve implant fixation and reduce the rate of revision surgery is through the development of a new generation of coatings with the ability to deliver osteostimulative agents to the bone-implant interface.

Bioactive glasses are a candidate material for this approach. When exposed to physiological fluids, the glasses leach silicon and other cations that lead to the formation of a silica gel onto which a calcium phosphate-rich layer precipitates. This calcium phosphate-rich layer permits protein adsorption (e.g., osteonectin, fibronectin, and vitronectin), encouraging cellular attachment, proliferation, and bone formation.[5–7] The ability to produce a calcium phosphate-rich layer enables bone bonding as well as the application of bioactive glasses as bone graft substitutes. However, in contemplating enhanced implant fixation, the role of bioactive glass dissolution products is of potentially greater interest. These demonstrate properties that are described as osteostimulative, promoting the growth, maturation, and activity of osteoblasts.[8–13] A further advantage of bioactive glasses is the ability to modify the glass composition through the substitution of calcium (or other constituent cations) for other cations that can alter the properties of the glass or be released through dissolution. The use of strontium within a bioactive glass is a promising strategy with the aim of enhancing local osteogenesis after implantation. Strontium, in the form of strontium ranelate, is an established therapy for osteoporosis, enhancing bone-forming osteoblast function while inhibiting bone-resorbing osteoclast activity.[14] We have shown *in vitro* that strontium-substituted bioactive glasses (SrBG) can be synthesized which up-regulate the anabolic role of osteoblasts, as measured by alkaline phosphatase activity, while reducing osteoclast tartrate-resistant acid phosphatase activity and decreasing osteoclast resorption of calcium phosphate films in a strontium dose-dependent manner.[15,16]

In earlier studies, bioactive glass coatings have been prone to mechanical failure at the implant-coating interface due to a mismatch in the thermal expansion coefficient (TEC) between the implant and coating material.[17] Attempts to match the TEC of bioactive glasses with common implant materials such as Ti6Al4V have tended to neglect factors such as crystallinity and network connectivity that have an impact on glass solubility and, consequently, its biological activity.[18,19] Therefore, an important

aim is to achieve an amorphous or low crystallinity glass with a network connectivity of less than 2.4[20] and to assess its potential as a new coating to enhance bone formation around an implant through combining the bone-forming effects of strontium and bioactive glass.

Materials and Methods

Glass synthesis

Glass was produced by mixing analytical-grade silica (Prince Minerals Ltd) with $CaCO_3$ (3.18 Mol. %), $SrCO_3$ (51.45 Mol. %), MgO (8.67 Mol. %), Na_2CO_3 (4.62 Mol. %), K_2CO_3 (4.62 Mol. %), ZnO (3.47 Mol. %), and $Ca_3(PO_4)_2$ (5.20 Mol. %) (all Sigma-Aldrich). The mixture was melted in a 300 mL platinum crucible at 1450°C for 1 h before quenching in water. The frit was dried overnight at 120°C and milled in a ball mill (Pulverisette; Fritsch GmbH). The milled glass was passed through sieves with particles greater than 50 µm, re-milled, and those particles less than 20 µm were discarded. The size of the glass particles was measured using a Cilas 1064 laser particle-size analyzer to ensure that the size distribution of the glass approximated to that of the HA (Captal 30; Plasma Biotal Ltd).

Implant preparation

Ti6Al4V cylinders that were 3.5 mm in diameter and 6.2 mm in length were grit blasted with alumina, ultrasonically washed, and plasma sprayed with either HA (Captal 30; Plasma Biotal) or SrBG to a coating thickness of 50–100 µm. Surface roughness was measured with a Wyko white light interferometer NT 9100 (Veeco) (SrBG R_a 11.9 µm, HA R_a 7.0 µm). Implants were sterilized in individual vacuum-sealed polyethylene packets by gamma irradiation at 35kGy (Swann Morton).

Differential scanning calorimetry

50 mg of SrBG powder with particle sizes of 20–50 µm was placed in a platinum crucible and analyzed by using differential scanning calorimetry (DSC) with analytical-grade alumina powder as a reference material. The experiments were carried out in air, using a Stanton–Redcroft DSC 1500 (PL Thermal Sciences), at different heating rates (5, 10, and 25 K min^{-1}) for an approximate maximum temperature of 1050°C, and the glass transition temperature (T_g) was determined.[21]

Dilatometry

The TECs for produced glasses were measured in a calibrated dilatometer (Netzch GmbH). The 25 mm-long glass bar samples were analyzed between 30°C and 500°C at a rate of 10°C/min. TEC (α) values were determined using the system software from the gradient of the TEC curve ($\alpha=[\Delta l/l_0]/\Delta T$), where Δl=change in length, l_0=original length, and ΔT=change in temperature.

X-ray diffraction

X-ray diffraction patterns of the glass powder and its plasma-sprayed coating on Ti6Al4V substrate were determined using an X-ray powder diffractometer

(PANanalytical X'Pert Pro MPD). This was performed with Ni filtered Cu-Kα radiation at a wavelength of 1.54Å. The diffraction pattern was recorded between 2θ values of 10°–80° with a step size of 2θ=0.04°.

Network connectivity

NC calculation was performed as described in.[22]

Ion-release profile

Dissolution studies were carried out on SrBG. 75 mg of <38 μm glass powders were immersed in 50 mL tris-buffer solution at pH 7.25. The soaked materials were placed in an orbital shaker incubator (New Brunswick Scientific C24 Incubator) at a constant temperature of 37°C for time periods of 0.5, 1, 2, 7, 14, 21, and 28 days. The glass powders were withdrawn from the solution by filtering through medium porosity filter paper (5 μm particle retention, VWR International). The obtained solutions were filtered (0.2 μm cellulose acetate syringe filters, Anachem) and maintained at 4°C. Samples were diluted by a factor 1:10 (for analysis of silicon (Si), calcium (Ca), strontium (Sr), phosphorus (P), and magnesium (Mg)) and quantitatively analyzed by inductively coupled plasma-optical emission spectroscopy (ICP-OES) (iCAP 6000; Thermo Scientific) with each sample read in triplicate.

In vivo study

Animal experiments were performed by the approval of the United Kingdom Home Office (Project licence PPL 70/7012). Twenty-seven 3.5–3.8 kg 6 month-old male New Zealand White rabbits underwent bilateral press-fit implantation of cylinders into both the medial femoral condyle and the proximal tibia under general anesthesia. Continuous saline irrigation was utilized during drilling to prevent thermal injury. A randomized limb of each rabbit contained bioactive glass implants, whereas the other contained HA. Wounds were closed in layers with 3-0 Vicryl and 3-0 Nylon used for skin. Sutures were removed at 10 days postoperation. Antibiotic prophylaxis (Baytril, Bayer) was provided for 5 days postoperatively. Regular analgesia was administered (Buprenorphine, Reckitt Benckiser) postoperatively for at least 3 days. Animals were caged individually with no restriction on activity. Food and water were provided *ad libitum*. The animals were sacrificed in equal groups of nine at 6, 12, and 24 weeks.

Mechanical testing

Tibial samples were dissected to completely expose both ends of the implant. A thin layer of PMMA was set around each implant to improve stability. Samples were prepared within 6 h of sacrifice and kept moist throughout testing. Push-out testing was performed using a screw-driven material testing machine (Instron) with a crosshead speed of 1 mm/min. Maximal pushout force was measured, and a value for maximal shear strength was calculated for the cylindrical surface of each sample.

Histology

Femoral samples were fixed in 10% v/v neutral-buffered formalin for 7 days before dehydration in graded ethanol and embedding in PMMA resin. The embedded

samples were sectioned parallel to the long axis of the implant using a Leica SP1600 microtome with a 270 μm diamond-edged blade with a 1:1 v/v mixture of glycerine and water as a lubricant and coolant. An initial thick section was produced for scanning electron microscopy. Three sections were obtained after exposure to 0.1 M HCl for 15 s, methylene blue for 60 s, and basic fuchsine for 30 s. A coverslip was glued to the tissue block with a UV-activated cyanoacrylate-based cement (301 Industrial Permacol Contact Cement) before each section. Bone-implant contact and bone to total volume within one high power field (500 μm) along the long edges of the implant were quantified using Osteomeasure software (OsteoMetrics). The mean value, for each parameter, of the three sections was used as the value for statistical analysis.

Scanning electron microscopy

Femoral samples embedded in PMMA resin were ground with 1200 grit SiC paper and polished with a 1 μm diamond suspension. A chromium sputter coating was applied to the samples at 1.2 atm pressure and 20 mA voltage for 4 min. A scanning electron microscope (LEO 1525) at 20 kV was used with EDX analysis.

Statistical analysis of in vivo data

A Wilcoxon Sign Rank Test was used to compare HA and SrBG groups at each time point. Variations between time points were analyzed with the Mann–Whitney *U* Test. All tests were undertaken at a 95% confidence level. All analysis was undertaken using SPSS 17 (SPSS, Inc.).

Results

A candidate SrBG with in vitro biological activity and material properties suitable for implant coating

We developed a bioactive glass in the system SiO_2-Na_2O-K_2O-CaO-MgO-ZnO-P_2O_5 as a candidate for use as an implant coating. We conducted DSC to obtain thermal data on SrBG (Fig. 1A) that demonstrated two glass transition values which were most distinct when heated at 25°C/min. This is consistent with the concept of bioactive glasses consisting of a two-phase system comprising an amorphous silicate matrix glass phase with a dispersed amorphous orthophosphate glass phase.[23] Both of these glass transition temperatures are lower than the α→β phase transition of the common orthopedic implant material Ti6Al4V, which occurs between 955°C and 1010°C, a design feature that should prevent degradation of the mechanical properties of the implant.

Differences in the TEC between substrate materials and coating materials can lead to thermal stress concentration at the time of coating application, which can, in turn, lead to coating failure at the implant coating interface. However, HA, which is extensively used as a successful coating in orthopedics, has a TEC of 12×10^{-6} °C^{-1} that is higher than the TEC of titanium alloy ($9–10\times10^{-6}$ °C^{-1}).[24] A TEC of a coating above that of the implant metal will produce compressive stresses on the metal, potentially enhancing the mechanical properties of the implant surface. We designed the TEC of SrBG to be comparable with that of HA, between 300°C–500°C demonstrating a TEC value of 12.45×10^{-6} °C^{-1}.

Next, we measured the crystallinity of SrBG using X-ray diffraction (XRD). Bioactive ceramics with a crystalline structure demonstrate slower dissolution and, consequently, biological activity than amorphous (i.e., glassy) structures. XRD analysis of both SrBG powder before plasma spraying and of the plasma-sprayed SrBG coating showed an amorphous structure (Fig. 1B), indicating there were no crystals present. Network connectivity is defined as the average number of linkages for the elements other than oxygen that form the network backbone. This can be determined through calculation based on glass structure and for SrBG, it was 2.33.

To investigate the dissolution behavior of SrBG, the powder was immersed in a tris buffer solution (Fig. 1C). During the first week of immersion, rate variations were observed in the release of ions. The concentration of released Sr^{2+} rises rapidly within the initial 12 h, reaching 23 ppm with a steady increase to 184 ppm by 14 days before the rate of increase reduces attaining 210 ppm by 28 days. Ca^{2+} concentration increases in a similar fashion to Sr^{2+} but at lower concentrations, reaching 20 ppm at 7 days and 68 ppm at 14 days before the rate tails off with a concentration of 78 ppm at 28 days. Strontium concentration increases more than the concentration of other ions after immersion of SrBG in tris buffer solution.

SrBG coating enhances early peri-implant bone formation

To investigate the *in vivo* performance of SrBG, we implanted grit-blasted Ti6Al4V cylinders, coated with either SrBG or a commercially available HA used for orthopedic implant coating, bilaterally into the distal femurs of twenty-seven New Zealand White rabbits. Animals were culled at 6, 12, or 24 weeks, with two animals excluded post mortem, one due to a subclinical infection at 6 weeks and one in the 24 week group, due to fracturing around an implant.

We produced thin (10 µm) undecalcifed sections of the distal femurs with sections orientated parallel to the long axis of the cylindrical implant to permit histological evaluation.[25] Interposition of fibrous tissue between the implant and bone was rarely seen, indicating implant stability and good biocompatibility of both coatings. Fibrous interposition between implant and bone was seen in one SrBG sample at 6 weeks (mean 28.5% of implant surface across the three sections), one SrBG sample at 12 weeks (mean 20.6% of implant surface), and two HA samples at 12 weeks (24.4% and 22.0% of implant surface). A thin layer (<10 µm) of SrBG was occasionally visible in 6 week samples (Supplementary Fig. S1i; Supplementary Data are available online at www.liebertpub.com/tea) and completely absent from later time points. HA was evident in all samples at all time points, but delamination of the coating was noted in one HA sample at 12 weeks. We are unable to determine whether this is an artefact of sectioning or a true failure of the coating (Supplementary Fig. S1ii).

A morphological difference in peri-implant bone between SrBG and HA sections was evident at 6 weeks (Fig. 2). The SrBG samples were associated with a thicker layer of bone adjacent to the implant compared with HA. The trabecular architecture was maintained adjacent to the implants in the HA sections with new bone deposited as an extension of the existing trabeculae. HA samples displayed more bone islands on the implant surface that were not linked to trabeculae (Supplementary Fig. S1iii), representing either *in contact* bone formation or extensions from trabeculae out of section. At later time points (12 and 24 weeks), the morphological differences between

the HA and SrBG groups reduced, with an increasingly organized mature trabecular architecture seen adjacent to the implants in both groups.

Quantitative analysis of the histological sections confirmed that the ratio of bone volume to total volume along the long sides of the implant and extending 500 μm from the edge of the implant or coating was significantly greater at 6 weeks in the SrBG group (p=0.017), and a trend for greater bone volume in the SrBG group was seen at 12 weeks (p=0.051) (Fig. 3). Peri-implant bone volumes in both groups reduced between 12 and 24 weeks, reflecting bone remodeling (SrBG p=0.038, HA p=0.038). Analysis of bone-implant contact showed no significant difference between the two groups at any time point.

We undertook a further evaluation of the bone implant interfaces of both HA and SrBG femoral implant sections using scanning electron microscopy (SEM) (Fig. 4 and Supplementary Fig. S2). SEM micrographs confirmed that the HA coating was present at all time points after implantation. However, the majority of the SrBG coating was absent by 6 weeks. SEM analysis was carried out on a sample from an animal culled at 10 days after implantation as a result of wound dehiscence. SEM micrographs demonstrated that the SrBG coating was present at this time point, suggesting that the absence of coating was secondary to dissolution rather than stripping away of the coating at the time of implantation. The backscattered images demonstrate direct apposition of bone to the titanium implant surface in the SrBG sections. The HA coating interlocks with the roughened implant surface with bone growth over the coating surface.

A selection of unstained thick (>200 μm) HA and SrBG sections underwent analysis using Energy-Dispersive X-ray spectroscopy (EDX) in the region extending 100 μm from the edge of the coating/implant to investigate the fate of the strontium within the SrBG coating (Fig. 5 and Supplementary Fig. S3). At all three time points, the EDX spectra of the HA sections showed peaks consistent with elements such as calcium and phosphorus, while the EDX spectra acquired from the SrBG coating demonstrated the presence of elements found in bone, metallic elements from the Ti alloy, and peaks from silicon. Strontium was not detected in the bone adjacent to either HA- or SrBG-coated implants. However, it should be noted EDX is semi-quantitative, and the detection of elements present at low levels (e.g., 1%) or with overlapping peaks (such as silicon and strontium) can be difficult can be difficult.

Superior push-out strength of grit-blasted titanium alloy implants coated with SrBG compared with HA

As a further test of implant fixation, we performed pushout experiments on grit-blasted titanium implants which were coated with either HA or SrBG that were placed bilaterally in the proximal tibial metaphysis of the same 27 rabbits used for the histology study. There was a trend for increasing maximal shear strength over time in the SrBG group compared with the HA group, with a significant difference between the two coatings at 24 weeks (p=0.028) (Fig. 6). Visual analysis of the implants after testing revealed increasing quantities of adherent bone on the HA implants at each time point. No adherent bone was seen on the SrBG implants at 6 weeks; however, bone was increasingly present at 12 and 24 weeks.

Discussion

Joint replacement surgery is increasingly popular; however, with individuals living longer and undertaking more active lifestyles, significant challenges exist in ensuring the longevity of implant fixation. The greatest cause of revision surgery is aseptic implant loosening that occurs either through excessive motion of the implant due to inadequate fixation or through inflammatory and osteolytic processes occurring because of particulate debris within the bone-implant interface.[26] It is known that implant fixation into bone with reduced mineral density is associated with impaired metrics of osseointegration such as bone-implant contact and push-out strength.[27,28] Implants embedded within lower mineral density bone are more prone to micromotion that, ultimately, may lead to implant loosening and failure.[29] Approaches to enhancing orthopedic implant fixation aim at rapidly limiting implant micromotion and at providing a seal at the bone-implant interface to limit particle ingress generated by articulating bearing surfaces.

Strontium is a strong candidate in the search for interventions that will enhance peri-implant bone formation and bone density. Investigations on strontium use in implant fixation have been published by a number of groups, including through the use of oral supplementation with strontium ranelate, incorporation into a titanium oxide layer, strontium-HA coatings, and nano-tube arrays.[27,30–35] These studies have consistently shown the beneficial effects of strontium on implant fixation. The combination of strontium with bioactive glass is an approach that combines the beneficial effects of strontium with the osteostimulative potential of bioactive glass dissolution products.

Previous attempts to develop bioactive glass coatings have failed for a variety of reasons, in particular through mismatched TECs, glass crystallization, and poor network connectivity.[18,19] The SrBG described in this article has addressed these issues through the production of a coating with a TEC similar to HA, an amorphous structure, and an acceptable network connectivity.

The traditional philosophy for coating metallic implants is to provide an intermediate layer between the inorganic implant surface and organic bone. HA provides this by bonding to the bone; however, it does not bond strongly to the implant surface. Instead, HA relies on close apposition to the implant surface with implant surface roughness, produced through a technique such as grit blasting, to provide a key.[36] The SrBG described in this article functions in a different way, sacrificing its function as a scaffold to maximize osteostimulation through the release of dissolution products, including strontium, at the bone-implant interface. This approach is similar to the use of agents such as the bone morphogenetic proteins to enhance implant fixation but at a much lower cost and better safety profile.[37] Similar to HA, this enhanced bone formation technique depends on the use of an implant substrate with a rough surface, porosity, or intrinsic osseointegrative potential, such as titanium, to maintain long-term fixation.[38]

Our data demonstrate that it is possible to increase early (6 week) bone formation around SrBG-coated implants compared with HA and that fixation of implants by 24 weeks is superior with SrBG on mechanical testing. The mechanism behind the enhanced maximal shear strength demonstrated at 24 weeks is not fully explained by this work and is an area for further investigation. Bone-implant contact is widely

believed to be the most important determinant of implant fixation, but no significant difference was found between HA and SrBG at any time point. One hypothesis is that a relative increase in peri-implant bone mineral density in the SrBG samples enhances the strength of trabecular attachments without necessarily increasing their volume. Bone densitometry is unreliable in the presence of strontium, and we were unable to obtain meaningful measurements of bone hardness due to the need to infiltrate the samples with resin during the sectioning process.

Surface finish has an impact on implant fixation; however, controlling this when comparing relatively rapidly and slowly degrading coatings is difficult. Initial surface roughness values for SrBG, which were higher than for HA, are unlikely to be particularly relevant due to the rate of dissolution, although we cannot exclude any impact from the exposure of the roughened titanium alloy surface. The aim in comparing SrBG to HA was to assess the merits of SrBG relative to the gold standard treatment in orthopedic surgery using an identically prepared implant, and this has been achieved. The further investigation of this SrBG will include a comparison to uncoated implants and the use of a weight-bearing model that assesses the impact of cyclical loading on implant fixation.

The data presented in this article show the potential for smart biomaterials to enhance implant fixation. We have shown that bioactive glasses can be synthesized to maximize their osteostimulative role without compromising on key material properties such as TEC which permit their use as coatings. This work demonstrates preclinical proof of concept with regard to the use of SrBG as an implant coating material for use in implants with an appropriate surface preparation. This material may prove to be of significant benefit in the field of skeletal reconstructive surgery in reducing rates of aseptic loosening.

Acknowledgments

The authors are grateful for the assistance of Natasja van Dijk in the production of the histological sections. We thank Prof. Robert Hill for useful discussions. We warmly thank Dr. Julian Jones for useful comments on the paper.

References

1. T. Jaeblon Polymethylmethacrylate: properties and contemporary uses in orthopaedics. J American Acad Orthop Surg 18**,** 297, 2010.
2. S.S. Rajaratnam, C. Jack, A. Tavakkolizadeh, M.D. George, R.J. Fletcher, M. Hankins and J.A. Shepherd Long-term results of a hydroxyapatite-coated femoral component in total hip replacement: a 15- to 21-year follow-up study. J Bone Joint Surg Br 90**,** 27, 2008.
3. Australian Orthopaedic Association National Joint Replacement Registry. Annual Report, Adelaide, AOA, 2010.
4. D. Ellams, M. Swanson and E. Young NJR Annual Report. Hemel Hempstead, UK, NJR, 2011.
5. A. El-Ghannam, P. Ducheyne and I.M. Shapiro Formation of surface reaction products on bioactive glass and their effects on the expression of the osteoblastic phenotype and the deposition of mineralized extracellular matrix. Biomaterials 18**,** 295, 1997.

6. A. El-Ghannam, P. Ducheyne and I.M. Shapiro Porous bioactive glass and hydroxyapatite ceramic affect bone cell function *in vitro* along different time lines. J Biomed Mater Res 36**,** 167, 1997.
7. A. El-Ghannam, P. Ducheyne and I.M. Shapiro Effect of serum proteins on osteoblast adhesion to surface-modified bioactive glass and hydroxyapatite. J Orthop Res 17**,** 340, 1999.
8. I. Xynos, A. Edgar, L. Buttery, L. Hench and J. Polak Ionic products of bioactive glass dissolution increase proliferation of human osteoblasts and induce insulin like growth factor II mRNA expression and protein synthesis. Biochem Biophys Res Commun 276**,** 461, 2000.
9. I. Xynos, A. Edgar, L. Buttery, L. Hench and J. Polak Gene expression profiling of human osteoblasts following treatment with the ionic products of Bioglass 45S5 dissolution. J Biomed Mater Res 55**,** 151, 2001.
10. I. Xynos, M. Hukkanen, J. Batten, L. Buttery, L. Hench and J. Polak Bioglass 45S5 stimulates osteoblast turnover and enhances bone formation *in vitro*: implications and applications for bone tissue engineering. Calcif Tissue Int 67**,** 321, 2000.
11. I. Christodoulou, L. Buttery, P. Saravanapavan, G. Tai, L. Hench and J. Polak Dose- and time-dependent effect of bioactive gel-glass ionic-dissolution products on human fetal osteoblast-specific gene expression. J Biomed Mater Res B Appl Biomater 74**,** 529, 2005.
12. M. Bossetti and M. Cannas The effect of bioactive glasses on bone marrow stromal cells differentiation. Biomaterials 26**,** 3873, 2005.
13. C. Loty, J. Sautier, M. Tan, M. Oboeuf, M. Jallot, H. Boulekbache, D. Greenspan and N. Forest Bioactive glass stimulates *in vitro* osteoblast differentiation and creates a favourable template for bone tissue formation. J Bone Miner Res 16**,** 231, 2001.
14. E. Bonnelye, A. Chabadel, F. Saltel and P. Jurdic Dual effect of strontium ranelate: Stimulation of osteoblast differentiation and inhibition of osteoclast formation and resorption *in vitro*. Bone 42**,** 129, 2008.
15. M.D. O'Donnell, P.L. Candarlioglu, C.A. Miller, E. Gentleman and M.M. Stevens Materials characterisation and cytotoxic assessment of strontium-substituted bioactive glasses for bone regeneration. J Mater Chem 20**,** 8934, 2010.
16. E. Gentleman, Y. Fredholm, G. Jell, N. Lotfibakhshaiesh, M. O'Donnell, R. Hill and M.M. Stevens The effects of strontium-substituted bioactive glasses on osteoblasts and osteoclasts *in vitro*. Biomaterials 31**,** 3949, 2010.
17. L. Hench and O. Andersson Bioactive glass coatings. In: L. Hench and J. Wilson, eds. An Introduction to Bioceramics. Singapore: World Scientific, 1993, pp. 239–259.
18. J.M. Gomez-Vega, E. Saiz, A.P. Tomsia, G.W. Marshall, and S.J. Marshall Bioactive glass coatings with hydroxyapatite and Bioglass particles on Ti-based implants. 1. Processing. Biomaterials 21**,** 105, 2000.
19. J. Gomez-Vega, E. Saiz and A. Tomsia Glass-based coatings for titanium implant alloys. J Biomed Mater Res 46**,** 549, 1999.
20. R. Hill An alternative view of the degradation of bioglass. J Mater Sci Lett 15**,** 1122, 1996.
21. N. Lotfibakhshaiesh, D.S. Brauer, and R.G. Hill Bioactive glass engineered coatings for Ti6Al4V alloys: influence of strontium substitution for calcium on sintering behaviour. J Non-Cryst Solids 356**,** 2583, 2010.
22. N. Ray Inorganic Polymers. London, UK: Academic Press, 1978, p. 130.
23. M.D. O'Donnell, S.J. Watts, R.V. Law, and R.G. Hill Effect of P_2O_5 content in two series of soda lime phosphosilicate glasses on structure and properties–Part I: NMR. J Non-Cryst Solids 354**,** 3554, 2008.

24. L. Sun, C. Berndt, K. Gross and A. Kucuk Material fundamentals and clinical performance of plasma-sprayed hydroxyapatite coatings: a review. J Biomed Mater Res 58**,** 570, 2001.
25. H. Van der Lubbe, C. Klein and K. De Groot A simple method for preparing thin (10 μm) histological sections of plastic embedded undecalcified bone with implants. Biotech Histochem 63**,** 171, 1988.
26. Y. Abu-Amer, I. Darwech and J.C. Clohisy Aseptic loosening of total joint replacements: mechanisms underlying osteolysis and potential therapies. Arth Res Ther 9 Suppl 1**,** S6, 2007.
27. L. Maïmoun, T. Brennan, I. Badoud, V. Dubois-Ferriere, R. Rizzoli and P. Ammann Strontium ranelate improves implant osseointegration. Bone 46**,** 1436, 2010.
28. I.N. Tsolaki, P.N. Madianos, and J.A. Vrotsos Outcomes of dental implants in osteoporotic patients. A literature review. J Prosthodontics 18**,** 309, 2009.
29. P. Trisi, G. Perfetti, E. Baldoni, D. Berardi, M. Colagiovanni and G. Scogna Implant micromotion is related to peak insertion torque and bone density. Clin Oral Implants Res 20**,** 467, 2009.
30. J. Park, H. Kim, Y. Kim, J. Jang, H. Song and T. Hanawa Osteoblast response and osseointegration of a Ti-6Al-4V alloy implant incorporating strontium, Acta Biomater 6**,** 2843, 2010.
31. J. Park Increased bone apposition on a titanium oxide surface incorporating phosphate and strontium. Clin Oral Implants Res 22**,** 230, 2011.
32. C. Chung and H. Long Systematic strontium substitution in hydroxyapatite coatings on titanium via micro-arc treatment and their osteoblast/osteoclast responses. Acta Biomater 7**,** 4081, 2011.
33. Y. Li, G. Feng, Y. Gao, E. Luo, X. Liu and J. Hu Strontium ranelate treatment enhances hydroxyapatite-coated titanium screws fixation in osteoporotic rats. J Orthop Res 28**,** 578, 2010.
34. Y. Xin, J. Jiang, K. Huo, T. Hu and P. Chu Bioactive $SrTiO_3$ nanotube arrays: strontium delivery platform on Ti-based osteoporotic bone implants. ACS Nano 3**,** 3228, 2009.
35. J. Park, T. Kwon and J. Suh The relative effect of surface strontium chemistry and super-hydrophilicity on the early osseointegration of moderately rough titanium surface in the rabbit femur. Clin Oral Implants Res 24**,** 706, 2013.
36. L. Nimb, K. Gotfredsen and J. Jensen Mechanical failure of hydroxyapatite-coated titanium and cobalt-chromium-molybdenum alloy implants. An animal study. Acta Orthop Belg 59**,** 333, 1993.
37. N. Epstein Pros, cons, and costs of INFUSE in spinal surgery. Surg Neurol Int 2**,** 10, 2011.
38. J. Baas, T. Jakobsen, B. Elmengaard, J.E. Bechtold, and K. Soballe The effect of adding an equine bone matrix protein lyophilisate on fixation and osseointegration of HA-coated Ti implants. J Biomed Mater Res Part A 100**,** 188, 2011.

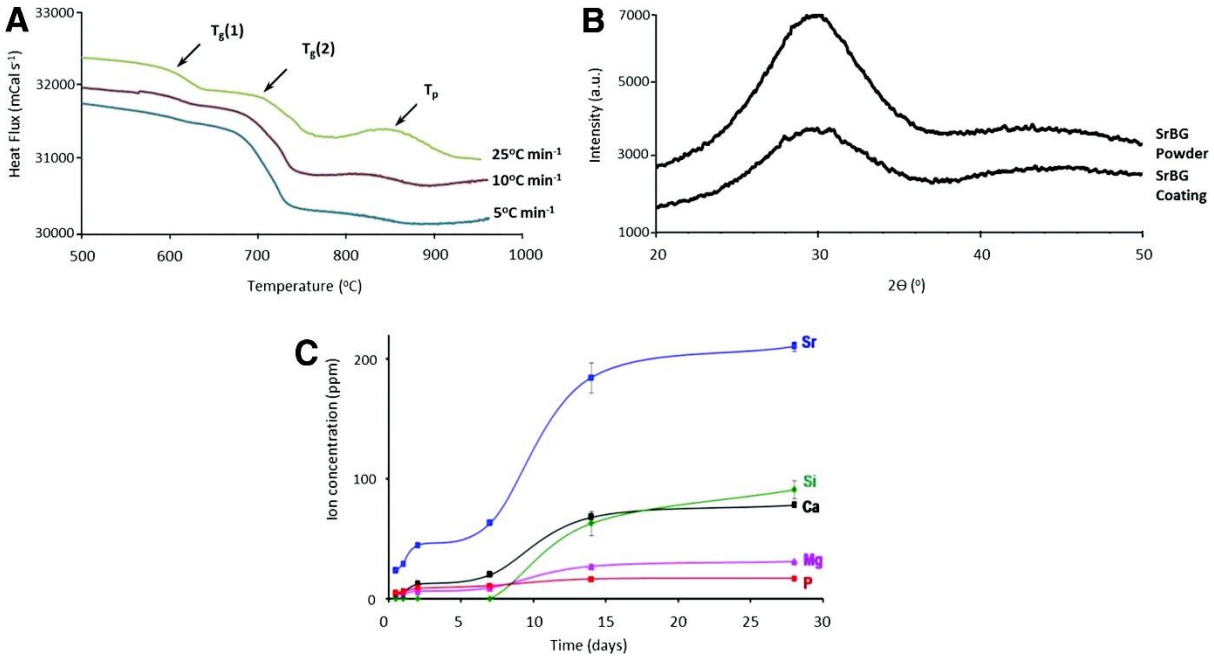

FIG. 1. Glass characterization studies. **(A)** Differential scanning calorimetry of strontium-substituted bioactive glass (SrBG) demonstrating two glass transition temperatures (T_g) and the glass crystallization temperature (T_p) that are most evident at a heating rate of 25°C min^{-1}. **(B)** X-ray diffraction analysis confirms that SrBG has an amorphous structure both before and after plasma spraying. **(C)** A dissolution study of SrBG in Tris buffer shows that the most marked dissolution of strontium and calcium occurs between 7 and 14 days, with a minimal further elevation in ion concentration subsequent to this.

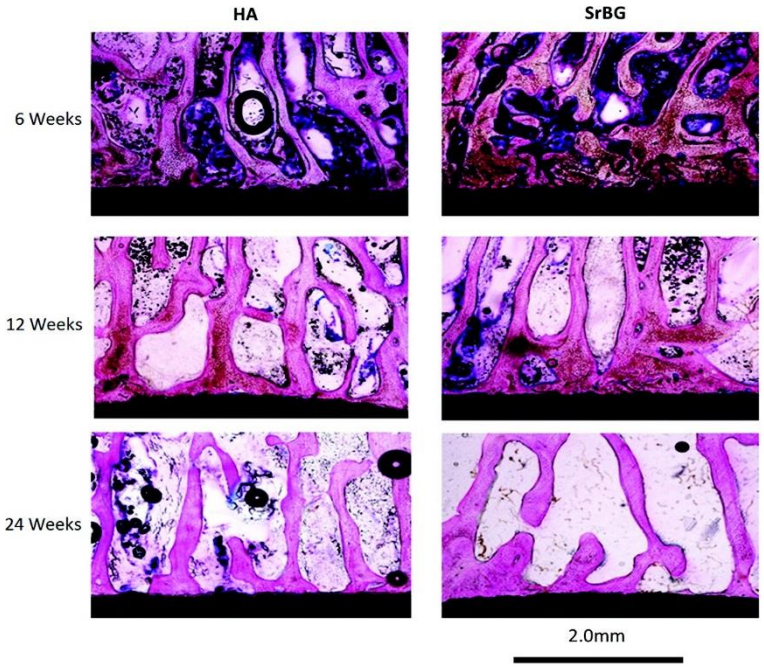

FIG. 2. Representative light microscopy sections of the femoral peri-implant region for both hydroxyapatite (HA) (left) and SrBG (right) at 6, 12 and 24 weeks

postimplantation stained with methylene blue and basic fuchsine. Increased bone is evident adjacent to the implant surface at 6 weeks in the SrBG specimens compared with the HA specimens. Through a process of remodeling, the volume of bone in both groups reduces over the course of the experiment, resulting in similar peri-implant bone morphology at 24 weeks.

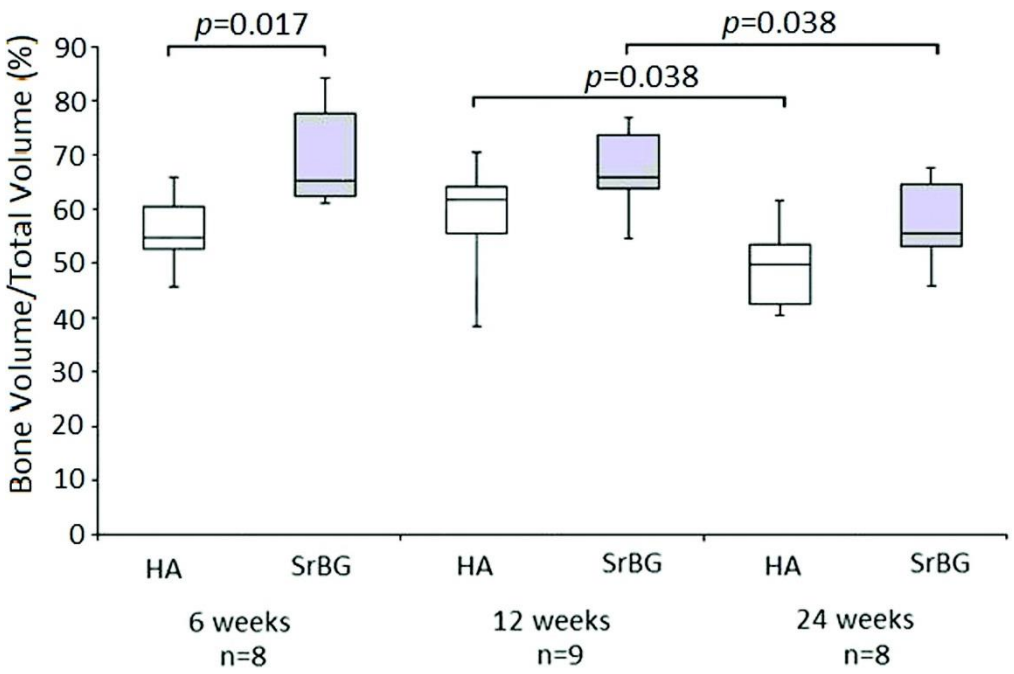

FIG. 3. Boxplot demonstrating the changes in the proportion of bone volume to total volume for HA- and SrBG-coated implants at 6, 12, and 24 weeks postimplantation. Median, interquartile range, and range are displayed. Greater bone volume is evident surrounding SrBG-coated implants at 6 weeks compared with HA-coated implants. The volume of bone surrounding both SrBG- and HA-coated implants reduced between 12 and 24 weeks secondary to remodeling.

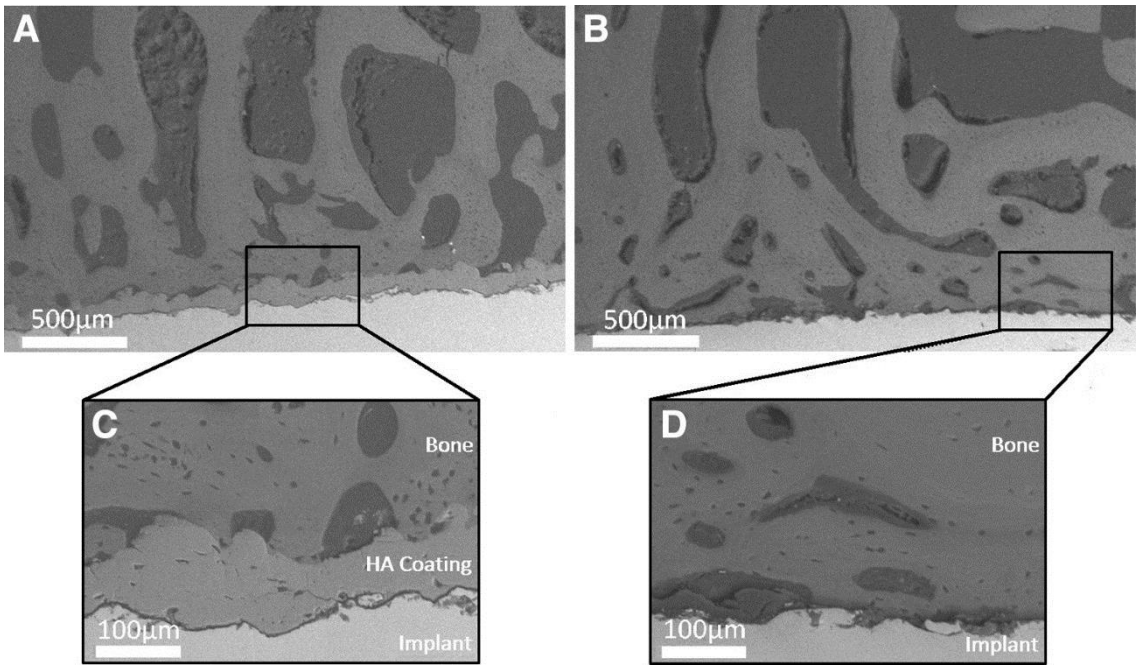

FIG. 4. Backscattered electron image of polished cross-sections of coated implants in femur at 6 weeks after implantation in the same animal; **(A)** HA-coated implant, **(B)** SrBG-coated implant, **(C)** bone-implant interface of HA-coated implant at higher magnification, and **(D)** bone-implant interface of SrBG-coated implant at higher magnification. SEM accelerating voltage=20 kV for all images. Bone apposition is evident to the Ti6Al4V implant surface and HA coating in the SrBG and HA samples respectively, with no evidence of SrBG coating.

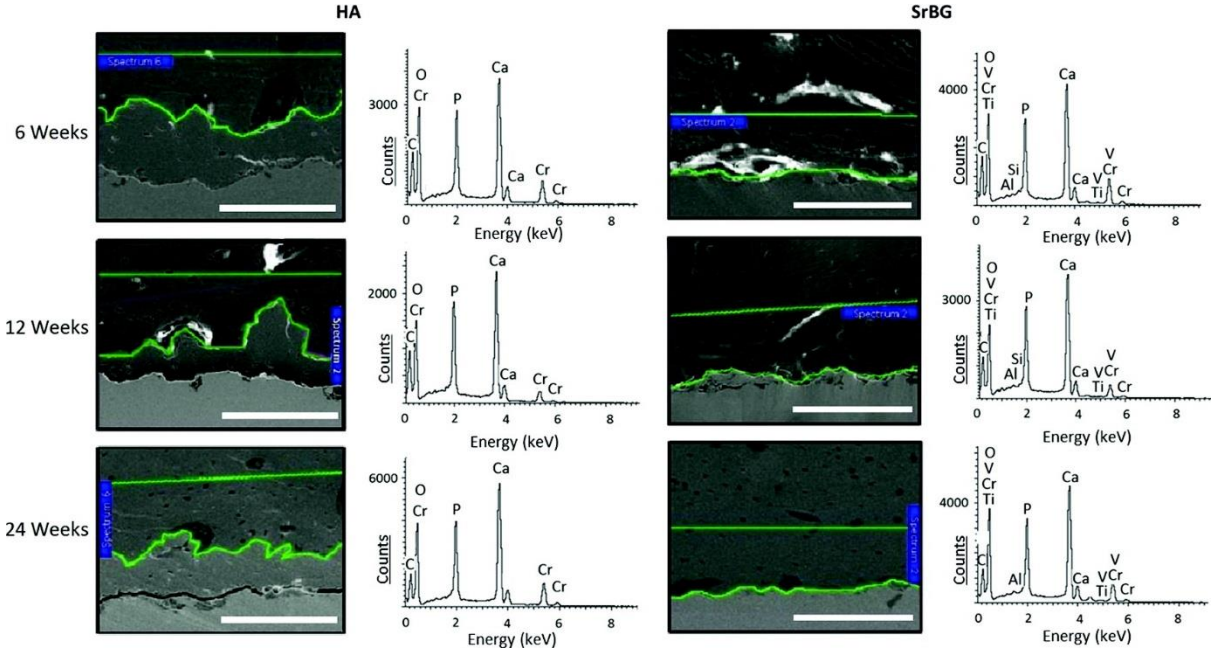

FIG. 5. Scanning electron microscopy (SEM) micrographs of polished cross-sections of implants in femur bone after 6, 12 and 24 weeks postimplantation; (left) HA-coated implants and (right) SrBG-coated implants. SEM micrograph for each time point from a single animal. The marked area corresponds to the area in which EDX analysis was performed; EDX spectra of the bone adjacent to the implants in femur bone at 6, 12, and 24 weeks after implantation demonstrated graphically with key elements present labeled. SEM accelerating voltage=20 kV. Scale bars=100 μm.

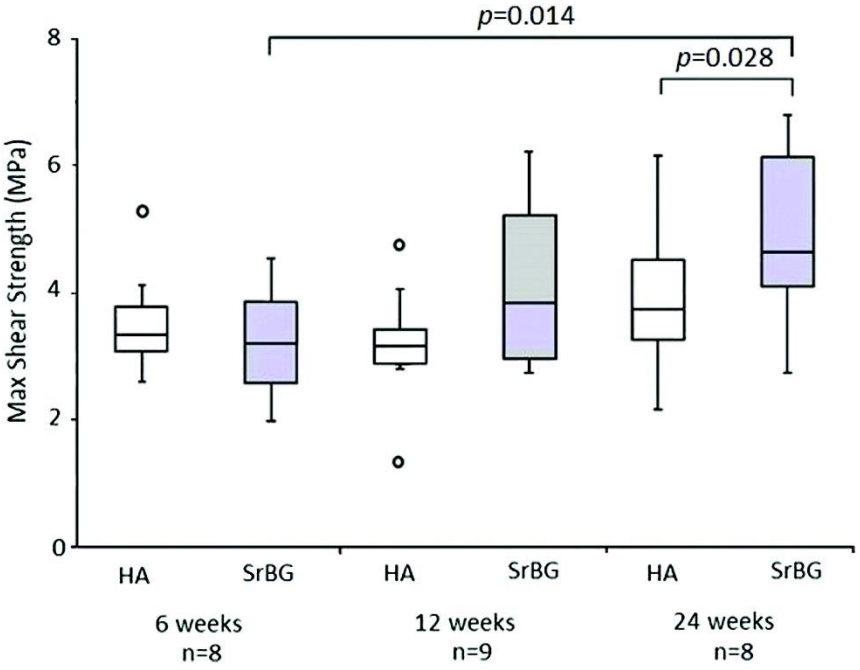

FIG. 6. Boxplot showing the maximal shear strength, median, outliers, and 25% and 75% percentile for HA- and SrBG-coated implants at 6, 12, and 12 weeks after implantation; **o** denote maximum and minimum outliers. A significant difference in maximal shear strength is evident at 24 weeks between SrBG and HA. Maximal shear strength increases between 6 and 24 weeks with SrBG, but a similar increase is not noted with HA.